Journal of Physics and Chemistry of Solids 71 (2010) 163–169

Contents lists available at ScienceDirect

Journal of Physics and Chemistry of Solids

journal homepage: www.elsevier.com/locate/jpcs

Effect of residual stress on the optical properties of CsCl thin films

Kuldeep Kumar [a], P. Arun [a,*], Chhaya Ravi Kant [b], N.C. Mehra [c], L. Makinistian [d,e], E.A. Albanesi [d,e]

[a] Department of Physics and Electronics, S.G.T.B. Khalsa College, University of Delhi, Delhi 110 007, India
[b] Department of Applied Sciences, Indira Gandhi Institute of Technology, Guru Gobind Singh Indraprastha University, Delhi 110 006, India
[c] University Science and Instrumentation Center, University of Delhi, Delhi 110 007, India
[d] Facultad de Ingeniería, Universidad Nacional de Entre Ríos, 3101 Oro Verde (ER), Argentina
[e] Grupo de Materiales Computacionales, INTEC-CONICET, Guemes 3450, 3000 Sante Fe, Argentina

ARTICLE INFO

Article history:
Received 18 March 2008
Received in revised form
6 September 2009
Accepted 22 October 2009

Keywords:
A. Thin films
C. X-ray diffraction

ABSTRACT

Large band gap alkali halides are known to have interesting optical properties. Though expected to be transparent in nature, defects in the crystal structure results in alkali halides having colors. The defects gives rise to new energy levels in the band structure, called color centers. Defects are easily generated on film fabrication and hence study of alkali halides promise to be interesting. In this manuscript we report the optical properties of cesium chloride (CsCl) thin films. We have correlated the optical properties of the films with the lattice size of the polycrystalline films, thus highlighting the strong relationship between the structure and optical properties of alkali halide films.

1. Introduction

Alkali halides (AH) were a topic of interest in the past for crystallographers involved in energy band structure calculations. Recently, interest in AH have been renewed in connection with their optical properties for device applications [1] and optical wave guides [2]. Due to solubility of CsCl in its thin film state, Yoshikawa et al. [3] did some limited amount of in situ characterization. Tsuchiya et al. [4] however took advantage of CsCl's high solubility and used its thin films as steam etchable resists in IC fabrication. With such new applications of AH and in particular CsCl thin films and the lack of any extensive study of these materials in its thin film state, we were encouraged to study the optical properties of cesium chloride in thin film state for the present work. The present work details the structural, morphological and optical spectrum analysis done on cesium chloride films.

To relate our experimental findings, we have also theoretically modeled the CsCl system. For our calculations we used the full-potential linearized augmented plane wave (FP-LAPW) method within the density functional theory (DFT), as implemented by the WIEN2k code [5]. It is a very accurate first-principles scheme for modeling the properties of materials. In our calculations, We have used the so-called generalized gradient approximation (GGA) [6,7], in the formal parametrization scheme of Perdew–Burke–Ernzerhof (PBE) [8,9]. This corrected function is semi-local and thus more sensitive to non-spherical components of the density, resulting in a better performance than the local density approximation (LDA) when applied in a full potential scheme like the WIEN2k. However, it has to be emphasized that both LDA and GGA always yield underestimated band gaps. The standard method for correcting this is to use the scissors operator [10], which basically adds a constant potential to the under-estimated band gap so as to reproduce the experimental values. This method is particularly used in the determination of the band gap which appear while considering interfaces between different semiconductors [11,12], in optical transitions [13], and when properties of bulk material are studied under the influence of pressure [14]. We have used this method in our results of densities of states and shifted up the regions above the Fermi energy by a constant value of 2.45 eV.

2. Experimental

Thin films of cesium chloride were grown by thermal evaporation using 99.98% pure starting material obtained from Loba Chemie Pvt Ltd., Mumbai. The films were grown on microscopic glass substrates maintained at room temperature. The films were grown at vacuum better than 10^{-6} and 10^{-7} Torr. Films grown by this method were found to be slightly translucent with a bluish or bluish-green tinge depending on the films thickness. The films were immediately kept in a desiccator on removal from the vacuum chamber. All our studies were completed within five days of sample fabrication.

* Corresponding author. Tel.: +91 11 29258401; fax: +91 11 27666220.
E-mail address: arunp92@physics.du.ac.in (P. Arun).

0022-3697/$ - see front matter © 2009 Elsevier Ltd. All rights reserved.
doi:10.1016/j.jpcs.2009.10.013

3. Results and discussion

3.1. Structural and morphological studies

Structural studies of the films were done using X-ray diffractometer (Philips PW 3020). The as grown films of CsCl were found to be polycrystalline in nature without exception. Characterizing peaks were found between $2\theta = 20-50^{\circ}$ (Fig. 1). The peak positions match those listed in ASTM Card no. 05-0607 confirming the films to be that of CsCl. Cesium chloride exists in simple cubic state with a chlorine atom at the center of the cube and one cesium atom at every corner of the unit cell [15]. The first peak is located around 21.55° is Miller indexed as (1 0 0). Hence, the inter-planar spacing or the "*d*" value of this peak is the lattice constant of unit cell itself. The size of the grains present in the polycrystalline films can be calculated using the full width at half maximum (FWHM) of the X-ray diffraction peaks. This calculation is done using the Scherrer relation [16],

$$D = \frac{0.9\lambda}{B\cos\theta} \tag{1}$$

where D is the grain size (Å), B is the FWHM of the particular peak, θ (rad) is the Bragg's angle and $\lambda(\sim 1.5405\,\text{Å})$ is the wavelength of X-ray.

The surface morphology of the films were examined using JEOL (JSM)-840 scanning electron microscope (SEM). This method gives the size of the grains lying on the surface. The grain size are measured using a scale calibrated to the length reference given by the electron microscope. The value reported here are averages of 10–15 grains selected randomly in the field of view of the micrograph. The grain size of the sample shown in the micrograph (Fig. 2) thus obtained was $4.30 \pm 0.02\,\mu\text{m}$. This is very different from the value obtained by Scherrer's relation (553 Å or 0.05 μm). This might be due to grain boundaries seen in SEM not enclosing prefect crystallites but volume where partial crystallinity exists or where crystallinity is evolving. To resolve this, we have studied the samples using transmission electron microscope (TEM). Since electrons are absorbed as they travel through the film thickness, co-relation between grain size calculated from XRD and TEM are restricted to very thin film samples. Fig. 3 shows TEM micrographs of such as sample. The micrographs show grains in various stages of formation. The larger grains show tail like appendages which suggest spiral grain growth. The micrographs show the average grain size to be of 120 ± 3 nm. The grain size as

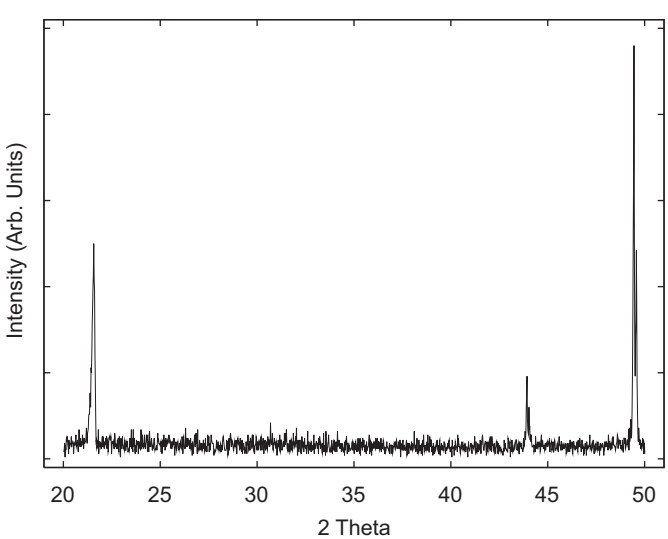

Fig. 1. X-ray diffraction pattern of a CsCl thin film studied.

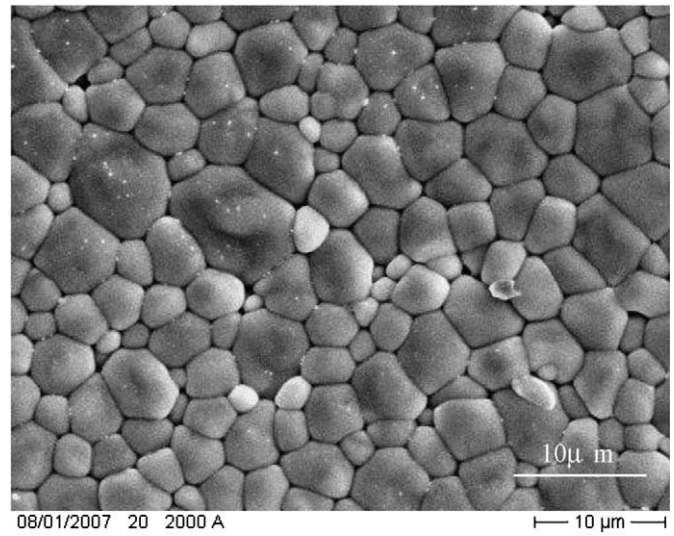

Fig. 2. The SEM micrograph of CsCl thin film. It can be observed that the grains of various sizes are densely packed throughout the film's surface.

evaluated from X-ray diffraction of the same samples is peaks of the order 75 ± 5 nm. The XRD results are in fairly good agreement with those obtained by TEM. However, the reduced estimate of grain size indicates that the X-ray peaks have broadened. Broadening of X-ray peaks also give information about the stress and defects in the film [17].

Following the methodology explained by Budakoti et al. [17], we have deconvoluted the broad X-ray peaks. Fig. 4 shows the deconvolutions done on the $2\theta \approx 21.55^{\circ}$ peak of some samples. Deconvolution was done using standard software like Origin 6. Deconvolution showed existence of two peaks, one at 21.55° and the second to the left. The peak at $2\theta \approx 21.55^{\circ}$ represents material having single crystal like structure while the second close peak represents material with defects in the crystal structure. These defects would play an important role in the optical properties of the film manifesting itself as stress in the film. In the following passages, we describe how we can quantify the influence of these defects in the optical properties of our films.

Broadening of X-ray peaks in thin films are usually accompanied with a shift in the peak position when compared to its position for single crystal of the sample. A displacement of the X-ray peak to the right as compared to peak position of single crystal indicate a decrease in *d*-spacing implying compressive stress acting on the film, vice versa the increase in *d*-spacing is indicative of tensile stress. The term "residual stress" (or simply stress) emphasizes the fact that the stress remains after all external forces are removed. These stresses acting in the film arises due to the very method of thin film deposition and can cause important effects on the properties of the material. The stress in the film is calculated after the strain in it is quantified using the relation

$$\frac{\Delta d}{d} = \frac{d_{obs} - d_{ASTM}}{d_{obs}} \tag{2}$$

where d_{obs} is the *d*-spacing measured for the thin film and d_{ASTM} is the corresponding peak's *d*-spacing of the single crystal as reported in the ASTM Card. The stress then can be determined by multiplying the average strain $\Delta d/d$ by the elastic constant of material. We have characterized our films with respect to strain since it is fundamental in nature (stress is calculated using this). The displacement of the X-ray peak to the left indicates tensile stress. Tensile stress is caused by vacancies [18], hence our

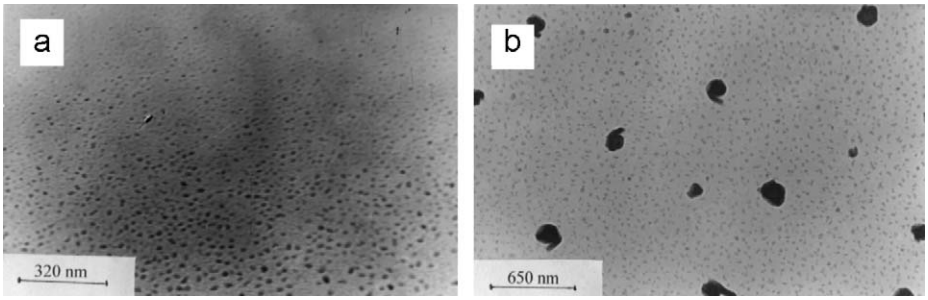

Fig. 3. Transmission electron micrographs of CsCl films taken at two different magnifications to exhibit uniform distribution of nanoparticles and different stages of grain formation.

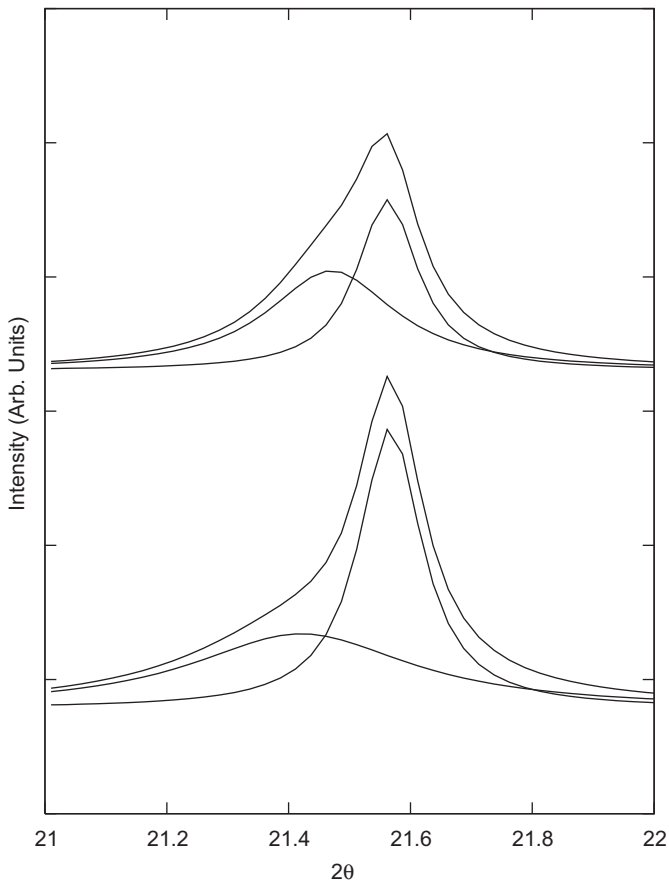

Fig. 4. Deconvolution of $2\theta \approx 21.55^{\circ}$ X-ray diffraction peak of two different samples show existence of defects in our CsCl films.

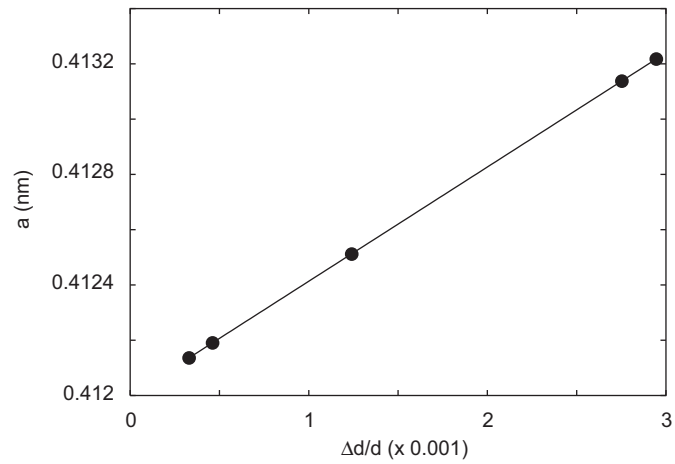

Fig. 5. The lattice size of the unit cell increases linearly with increasing tensile strain acting on the film. All the data points lie on the best fit line ($a = 0.413(\Delta d/d) + 0.412$) with a co-relation factor of 0.999.

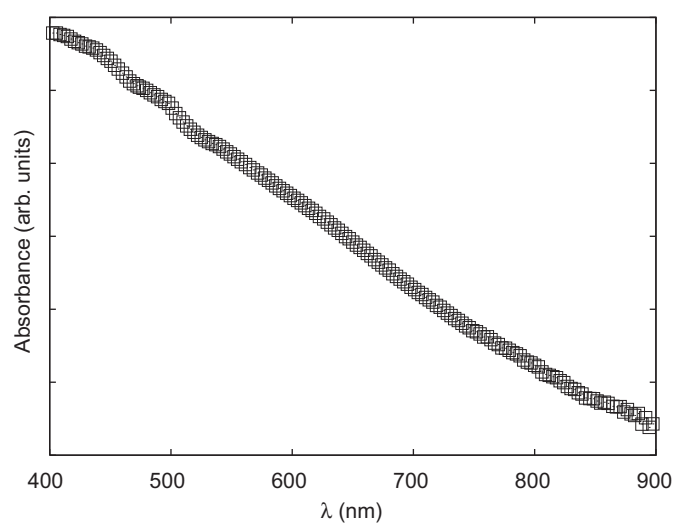

Fig. 6. The absorption spectra of CsCl film whose lattice constant from X-ray diffraction was found to be 0.4121 nm.

colored films suggest formation of color centers due to Cl vacancies. These vacancies leads to neighboring atoms stretching into it resulting in tensile stress.

The strain in the film decreased with increasing film thickness. The strain was found to directly influence the size of the unit cell or in other words the lattice constant (see Fig. 5). On extrapolating the best-fit line to the "*y*"-axis we get the lattice constant as 0.412 nm. This is the value reported in the ASTM card for a single crystal where zero strain is expected.

4. Optical studies

Alkali halide (AH) compound's crystals are usually transparent. However, vacancies in the compounds created by the absence of some halogen atoms are known to give their crystals color. These vacancies lead to appearance of energy levels within the forbidden gap. Transitions to and from these level's in turn gives rise to the color. In the literature such "color centers" are manufactured by X-ray irradiating AH crystals [19,20]. The fact that our films have bluish or bluish-green tinge suggest our

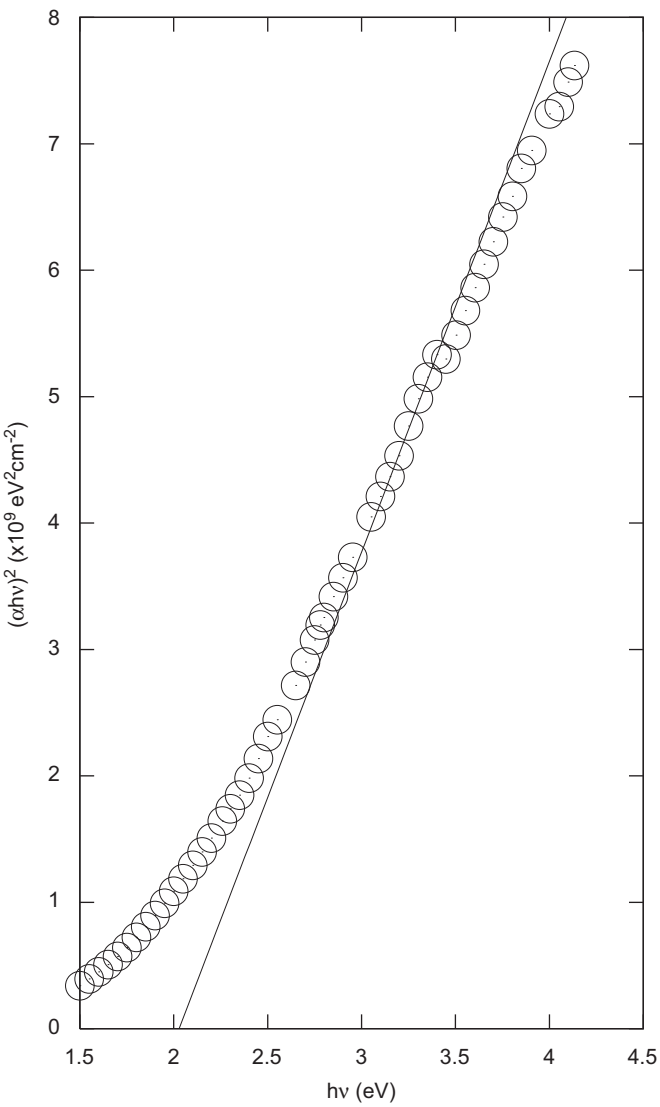

Fig. 7. The plot of $(\alpha h\nu)^2$ vs. $h\nu$ for the polycrystalline CsCl film whose absorption spectra is shown in Fig. 5. The straight line show the least square fitting used to determine E_o by extrapolation.

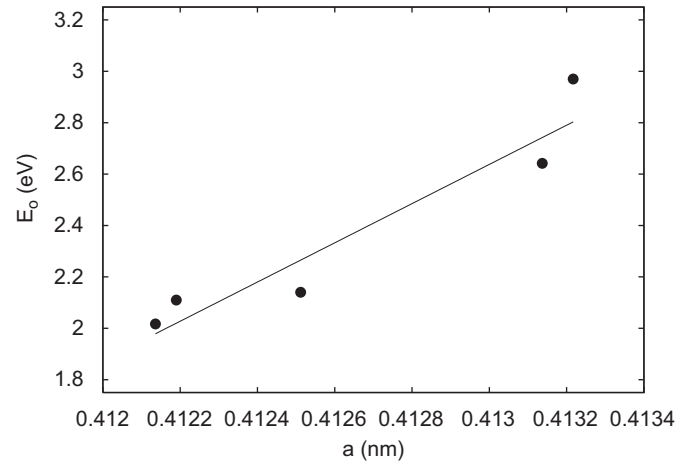

Fig. 8. The variation of the absorbance energy with lattice constants.

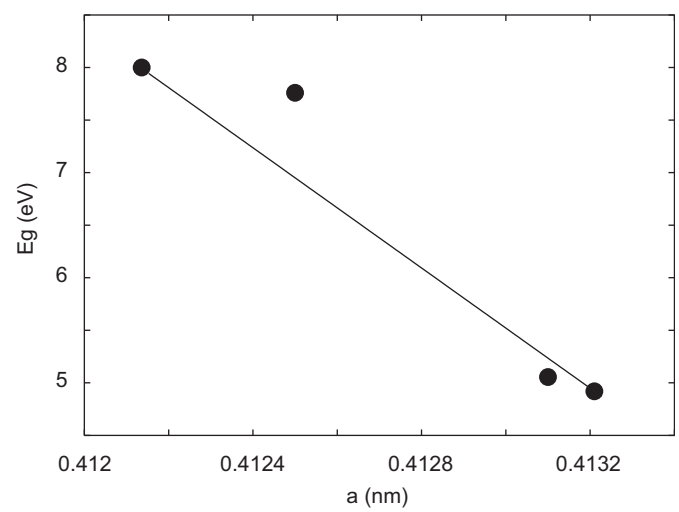

Fig. 9. The (estimated) band-gap of CsCl decreases with increasing lattice constant.

samples have chlorine deficiencies. Thus, we believe that the defects suggested by our structural analysis are caused by missing chorine atoms from the lattice. The color-centers were formed due to deposition of some dissociated AH molecules during thermal evaporation.

The absorption spectra of CsCl films showed increasing absorption as one proceeds to lower wavelengths. Such trend was reported by Rabin and Schulman [21] and Avakian and Smakula [22] in CsCl single crystals. It is on these sloped backgrounds they reported the appearance of peaks which represent the color-centers. In the referred works,color-centers were created by irradiating the single crystals with X-rays. In unirradiated samples, the peaks due to color-centers were too faint. Even for irradiated samples, the peaks were faint and became prominent only when the pre-irradiated absorption spectra was used as the baseline and subtracted from the spectra [21]. The color centers were characterized by the position of these peaks. However, these works do not comment on the sloped absorption background which also shows variation on X-ray irradiation.

4.1. Analysis of short wavelength absorption spectra

We carried out our optical studies using Shimadzu's UV 2501-PC UV–visible spectroscope. In Fig. 6 we show an representative absorption spectra of our film. As can be seen, we did not get any sharp and distinct peaks. Hence, we used the slope of the absorption spectra to comment on the nature of color centers. A slope in the absorption spectra is usually associated with multiple energy levels coming together forming bands. Assuming narrow bands are formed within the forbidden band due to color centers, we used Tauc's [23] for estimating band gap from the absorption spectra (near the band edge, $\lambda \sim 300-500$ nm) to determine the difference in energy level edge's (E_o) from the narrow bands arising due to color-centers to that of the conduction band. The variation in E_o determined as a function of lattice constant of the unit cell is shown in Fig. 8. Increasing lattice constant and inturn increasing strain gives rise to color-centers in the film. Since strain decreased with increasing film thickness one can appreciate the bluish tinge thin films having $E_o \sim 3$ eV while the bluish-green thick films have $E_o \sim 2$ eV associated with it's color-center. Thus our assumption of association between the absorption spectra's slope with color-centers is correct (see Figs. 6–8).

4.2. Analysis of long wavelength absorption spectra

The absorption edge of very large band-gap material like CsCl, lies in the UV region. Hence our absorption data can not be used to determine the energy band gap using the conventional Tauc's method [23]. However, an indirect estimation of the band-gap can still be made from the absorption spectra in a region far away from the band edge ($\lambda \sim 750-900$ nm). Such calculations have been carried out in other materials [24]. It has been shown that the optical absorption coefficient of semiconductors and insulators vary exponentially with incident photon energy away from the band edge [25]. The behavior is called the Urbach tail and the absorption coefficient is related to the photon energy as [26]

$$\alpha(E) = \alpha_o \exp^{((E_g - E)/E_u)} \tag{3}$$

where E_g is the extrapolated band-gap and α_o the absorption coefficient of the material at the band-gap energy. E_u is called the Urbach energy. The values of Urbach energy can be determined from the slope of the best fit straight line

$$\ln(\alpha) = \left[\ln(\alpha_o) - \frac{E_g}{E_u}\right] + \left(\frac{1}{E_u}\right)E \tag{4}$$

We have fit Eq. (4) on our absorption data and have estimated the values of E_u. Using this result, the band gap of the films were extrapolated from the intercepts obtained by fitting Eq. (4) to our data. *For these calculations, the value of absorption coefficient at band-edge, α_o was taken for bulk or very thick film* [21]. Estimated E_g shows a decreasing trend with increasing lattice constants (Fig. 9). The displacement of Cs and Cl atoms, moving away from each other with increasing lattice constant maybe the cause of decreasing band gap. Increasing atomic distances would decrease the effective lattice potentials as seen by the electrons producing change in band gap. *However, it has to be mentioned here that a small change in lattice parameter seems to produce a very large change in E_g. We believe the quantitative estimates here are erroneous since the value of α_o would also vary with varying film thickness and lattice parameter. Hence, the calculations at best gives a qualitative trend in variation. We now proceed to band structure calculations to substantiate these results.*

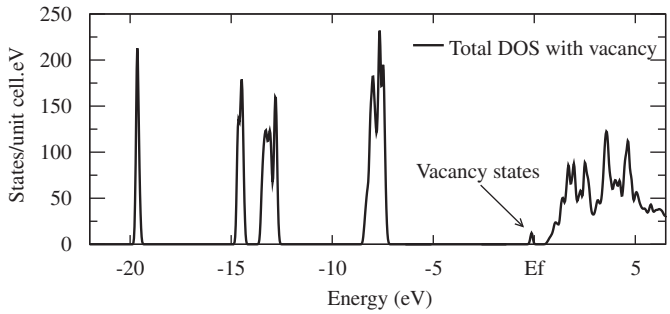

Fig. 10. Calculated density of states of the CsCl lattice with a Cl vacancy. The Fermi energy ($E_f = 0$ eV), is at the top of the impurity band (vacancy states) since that is occupied by the electrons that the chlorine vacancies release.

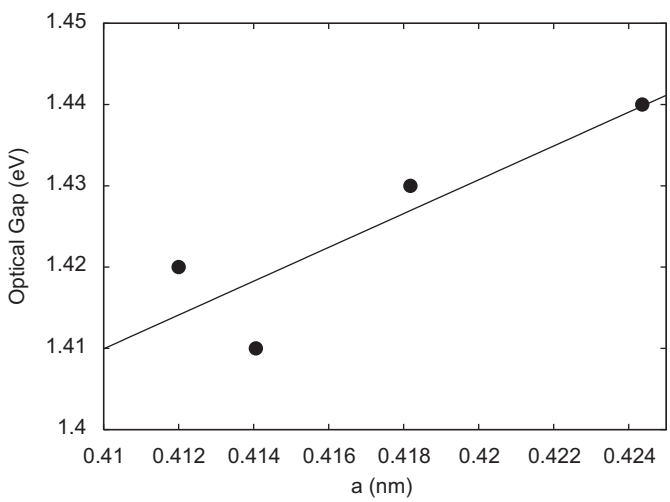

Fig. 11. Calculated optical energy gaps at different lattice parameters. The trend is in agreement to that shown in Fig 8. The data points represent theoretically calculated E_o, the difference between the localized state (F centers) to the first significant conduction band.

5. Band structure calculations

To qualitatively substantiate these results, we have modeled the defects in our poly-crystalline films, with a cubic super-cell of 53 atoms with a Cl vacancy in its center. That is, our super-cell

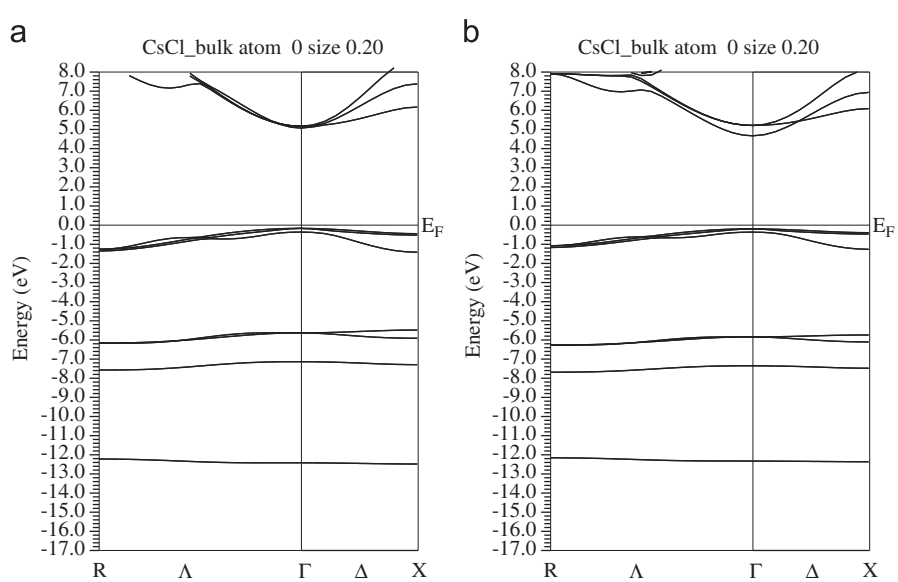

Fig. 12. Calculated band structures at (a) lattice constant of single crystal (0.4120 nm) and (b) of lattice constant 0.4236 nm, without vacancy. The scissor correction discussed in text has not been applied on the calculations of this figure.

consist of 27 unit cells in cubic array and the center most unit cell has a vacancy or in other words a chlorine atom missing in the center most unit cell of our super-cell. Fig. 10 shows the calculated density of states (DOS), where a flat band of localized states appears in the band gap, close to the bottom of the conduction band. These vacancy states are filled with trapped electrons, turning the films active in the visible region. We have used 89 k-points in the first Brillouin Zone in our calculations, which ensures a well converged electronic structure. The minimum energy differences (E_o) between these localized states to the first significant conduction band states are about 1.5 eV, and to the subsequent close first shoulders are about 1.6 and 2.1 eV, in close agreement with the experimental F-centers energy of about 2.0 eV for bulk [15] CsCl.

We have also calculated the energy position of the F-centers for different lattice parameter into the range at which our films were formed. The data points in Fig. 11 show theoretically calculated E_o for different lattice parameters. The figure only shows the minimum energy differences between the localized states to the first significant conduction band states. In all cases, however, there were close subsequent peaks up to about 2.0 eV (not shown in fig). We did not evaluate the possible values of E_o below 2 eV from the absorption spectra since the corresponding region would show signatures of the Urbach tail. In the Urbach tail region, the absorbance varies exponentially with the wavelength. The theoretical findings are however,in agreement with the experimental results (Fig. 8) of increase in E_o with increasing lattice size.

In Fig. 12, we compare the band structures of bulk CsCl with lattice parameters (a) of CsCl in single crystal state (= 0.412 nm) and (b) at 0.423 nm. The figure shows the region $R \rightarrow \Gamma \rightarrow X$ that forms the minimum gap. In both cases we have a direct transition band gap, located at the Γ point. This is in agreement with the calculations made on CsCl by Satpathy [27]. The main difference corresponds to the bottom of the conduction band at the Γ point, since at the equilibrium lattice constant three bands forming the bottom of the conduction band are degenerated at the Γ point, while at the higher lattice constant the degeneration is broken and a band splits down in energy, with the main difference of 0.37 eV at the Γ point. The breaking of degeneracy is observed in all simulations where the lattice constant is considered more than 0.412 nm. The variation in band gap with increasing lattice constant was theoretically simulated (see Fig. 13). The valence bands maintains its structure in all cases, although negligible differences can be observed for the top of the valence band in the Δ direction.

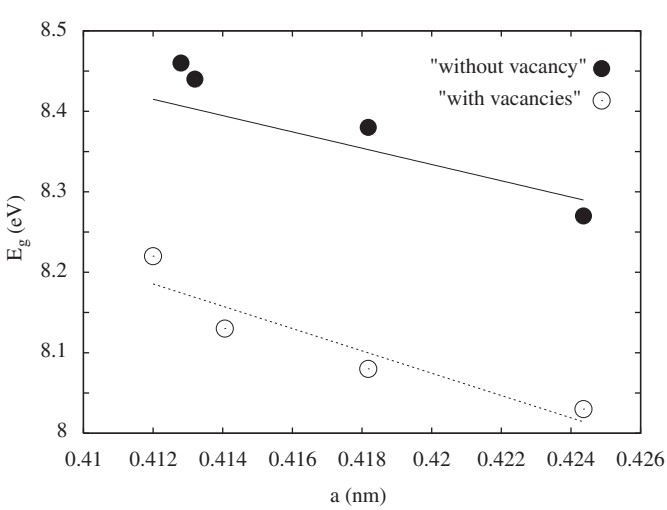

Fig. 13. The optical band-gap of CsCl decreases with increasing tensile stress. These results are after the application of scissor correction on calculations. Lines are only for visual aids to understand the trend.

The band-gap of CsCl single crystal as per our calculations works out to be 8.3 eV, in agreement to those reported in literature [28]. Repeated calculations for varying lattice parameters show the band-gap to vary. The theoretical calculations show a decreasing trend in band-gap with increasing lattice constant similar to our experimental results. However, Fig. 13 does not indicate a large variation in band-gap with lattice constant as indicated in Fig. 9. As stated earlier, our films were colored indicating the existence of vacancies in our films. Hence we repeated our calculations for band gap with one chlorine atom absent per 27 unit cells. Fig. 13 compares the two results. A chlorine atom vacancy in 27 unit cell leads to a reduction of 0.3 eV in the material's band gap. This variation is nearly constant throughout the range of increase in lattice constant studied. Discrepancy between theoretical and experimental results would essentially be due to larger vacancy concentration (than assumed for computation), that is varying with film thickness. However, the theoretical calculations do qualitatively corroborate the finding of our experimental studies. We have been able to derive valuable information from both the short and long wavelength regions of the optical spectra. In fact from the slope of the absorption spectra we have unconventionally used Tauc's method and been able to comment on the color-centers of our film, whose trend with film thickness/strain agrees qualitatively with computed results.

6. Conclusions

Alkali halide films have not been a popular area of research. Though they are wide band gap materials, colored crystals have been obtained. Similarly, though their films are expected to be transparent in nature, thin films of cesium chloride fabricated had light-blue to bluish-green tinge depending on the film thickness. This suggests the formations of color centers due to vacancies caused by absence of Cl atoms. This was found to depend on the film thickness. This enabled us to relate the band structure to the optical properties of the film. We believe our theoretical and experimental results are indicative of the material's behavior.

Acknowledgments

The help in completing the spectroscopic and diffraction analysis by Mr. Dinesh Rishi (USIC), Mr. Padmakshan and Mr. Rohtash (Department of Geology, Delhi University) is gratefully acknowledged. L.M. and E.A.A. acknowledge financial support from the Consejo Nacional deInvestigaciones Científicas y Técnicas (CONICET), the Universidad Nacional de Entre Ríos (UNER), and the Agencia Nacionalde Promoción Científica y Tecnológica (ANPCyT), Argentina. Author K.K. wishes to acknowledge the financial assistance from U.G.C. (India) in terms of Minor Project 6-1(222)/2008 (MRP/NRCB).

References

[1] S. Asaka, M. Itoh, M. Kamada, Phys. Rev. B 63 (2001) 081104.
[2] M. Cremona, J.A.M. Perira, S. Pelli, G.C. Righini, Appl. Phys. Lett. 81 (2002) 4103.
[3] G. Yoshikawa, M. Kiguchi, K. Ueno, A. Koma, K. Saiki, Surf. Sci. 544 (2003) 220–226.
[4] S. Tsuchiya, M. Green, R.R.A. Syms, Electrochem. Soild State Lett. 3 (2000) 44–46.

[5] P. Blaha, K. Schwarz, J. Luitz, Viena University of Technology, 2001. (Improved and updated version of the WIEN code, published by P. Blaha, K. Schwarz, P. Sorantin, S.B. Rickey, Comp. Phys. Commun. 59 (1990) 399.).
[6] J.P. Perdew, J.A. Chevary, S.H. Vosko, K.A. Jackson, M.R. Pederson, D.J. Sing, C. Fiolhais, Phys. Rev. B 46 (1992) 6671.
[7] J.P. Perdew, Y. Wang, Phys. Rev. B 45 (1992) 13244.
[8] J.P. Perdew, K. Burke, M. Ernzerhof, Phys. Rev. Lett. 77 (1996) 3865.
[9] J.P. Perdew, K. Burke, M. Ernzerhof, Phys. Rev. Lett. 78 (1997) 1396.
[10] M. Lanoo, M. Schllüter, L.J. Sham, Phys. Rev. B 32 (1984) 3890.
[11] S. Wey, A. Zunger, Phys. Rev. B 55 (1977) 13605.
[12] E.A. Albanesi, W.L. Lambrecht, B. Segall, J. Vac. Sci. Technol. B 12 (1994) 2470.
[13] R. Laskowski, N.E. Christensen, G. Santi, C. Ambrosch-Draxl, Phys. Rev. B 72 (2005) 035204.
[14] Z. Nabi, B. Abbar, S. Mecabih, A. Khalfi, N. Amrane, Comput. Mater. Sci. 18 (2000) 127.
[15] C. Kittel, Introduction to Solid State Physics, Wiley, NY, 1953.
[16] B.D. Cullity, Elements of X-Ray Diffraction, Addison-Wesley, New York, 1956.
[17] G.C. Budakoti, B. Kumar, G. Bhagavannarayana, N.C. Soni, Phys. Status Solidi A 202 (2005) R7–R9.
[18] W. Buckel, J. Vac. Sci. Technol. 6 (1969) 606.
[19] R.W. Pohl, Proc. Phys. Soc. London 49 (1937) 3.
[20] K. Przibram, Irradiation Colors and Luminescence, Pergamon Press, New York, 1956.
[21] H. Rabin, J.H. Schulman, Phys. Rev. 125 (1962) 1584.
[22] P. Avakian, A. Smakula, Phys. Rev. 120 (1960) 2007.
[23] J. Tauc, in: J. Tauc (Ed.), Amorphous and Liquid Semiconductors, Plenum, London, 1974.
[24] I. Bonalde, E. Medina, S.M. Wasim, J. Phys. Chem. Solids 66 (2005) 1865.
[25] F. Urbach, Phys. Rev. 92 (1953) 1324.
[26] M.V. Kurik, Phys. Status Solidi A 8 (1971) 9.
[27] S. Satpathy, Phys. Rev. B 33 (1986) 8706.
[28] R.T. Poole, J.G. Jenkin, J. Leisegang, R.C.G. Leckey, Phys. Rev. B 11 (1975) 5179.